

# **CONTROL OF MACRO-CELL AND MICRO-CELL CORROSION OF STEEL IN CRACKED CONCRETE**

## **Name and ID**

Abid Hasan Saumik, 180051114

Rifat Zaman, 180051119

Md. Sajjad Hossain Khan, 180051205

Md. Aktaruzzman Rony, 180051206

**A THESIS SUBMITTED FOR THE DEGREE OF BACHELOR  
OF SCIENCE IN CIVIL ENGINEERING (STRUCTURE)**

**DEPARTMENT OF CIVIL AND ENVIRONMENTAL ENGINEERING**

**ISLAMIC UNIVERSITY OF TECHNOLOGY (IUT)**

**2023**

# PROJECT APPROVAL

This is to certify that the thesis entitled “CONTROL OF MACRO-CELL AND MICRO-CELL CORROSION OF STEEL IN CRACKED CONCRETE” submitted by Abid Hasan Saumik, Rifat Zaman, Md. Sajjad Hossain Khan and Md. Aktaruzzaman Rony has been approved as partial fulfillment of the requirement for the Degree Bachelor of Science in Civil Engineering at the Islamic University of Technology (IUT).

Supervisor



---

**Dr. Md. Tarek Uddin, P.Eng.**

Professor

Department of Civil and Environmental Engineering (CEE)


Islamic University of Technology (IUT)


Board Bazar, Gazipur-1704, Bangladesh.


# DECLARATION


We declare that the undergraduate research work described in this thesis was completed by us under the expert supervision of Professor Dr. Md. Tarek Uddin. The appropriate cautionary measures have been taken to guarantee that the work being done is unique. The material presented here has not been copied, plagiarized or placed elsewhere for any reason other than publication.

## Name and ID

Abid Hasan Saumik, 180051114 

Rifat Zaman, 180051119 

Md. Sajjad Hossain Khan, 180051205 

Md. Aktaruzzman Rony, 180051206 

# DEDICATION

We dedicate our thesis to our parents, who over a long period of time gave us their important time, means of support, and labor so that we may become who we are today. They have inspired and supported us, enabling us to pursue our technical goals without ever looking back. They have our eternal gratitude.

We also want to convey our sincere appreciation to Professor Dr. Md. Tarek Uddin, our respected supervisor, for his continuous encouragement and motivation. Without him, this endeavor would not have been possible.

# ACKNOWLEDGEMENT

*"In the name of Allah, Most Gracious, Most Merciful"*

Our gratitude is to Almighty Allah for blessing us with a chance to complete this thesis and for enabling us in resolving issues that emerged throughout our project work.

We would like to express our sincere appreciation to our supervisor, Dr. Md. Tarek Uddin, P.Eng., Professor, Department of Civil and Environmental Engineering, Islamic University of Technology, for his kind supervision, helpful advice, and continuing support. His creative and technical guidance was essential to the success of this research project. The paper would never have been completed without his help and direction.

Furthermore, we have our mindful gratitude to all the faculty members for their meaningful recommendations throughout this thesis work. We would like to express our gratitude to the Lab Instructors for their assistance and support.

## ABSTRACT

A scientific investigation on controlling macrocell and microcell corrosion of steel bars in cracked concrete made with slag cement types B (SC-B) and slag cement type C (SC-C) was performed for a total of seven cases. Two control cases, one for SC-B and another one for SC-C were also investigated. Cement and lime-coated steel bars were used to control corrosion, along with the injection of lime slurry into the cracked region. Prism specimens were made for each of the cases. The prism specimens were made using a segmented steel bar that allowed for an external electrical connection. This connection was required for measuring the macro-cell and micro-cell corrosion currents. For the first 30 days, the specimens were submerged in seawater and continuously exposed to it. After that, the specimens were subjected to five cycles of submerging followed by drying at two-day intervals. Throughout this time, a data logger was used to record and monitor the voltage drop. Half-cell potential and depth of the corrosion were also studied. The experimental results show that when submerged in seawater, SC-C cement concrete outperforms SC-B cement concrete in terms of corrosion resistance. Lime treatment decreases corrosion current and improves corrosion resistance in SC-B cement concrete and SC-C cement concrete. Steel bars coated in lime and cement performed better than the uncoated steel bars of SC-B. The most efficient approach for avoiding corrosion is to treat SC-C cement concrete with lime slurry before immersing it in seawater.

**Keywords:** *macrocell corrosion, microcell corrosion, half-cell potential, corrosion depth, lime slurry, slag cement, rebar coating.*

# Table of Contents

PROJECT APPROVAL.....	ii
DECLARATION.....	iii
DEDICATION .....	iv
ACKNOWLEDGEMENT .....	v
ABSTRACT .....	vi
CHAPTER 1: INTRODUCTION.....	11
1.1    General .....	11
1.2    Background.....	12
1.3    Objectives of the study.....	13
1.4    Research Flow Diagram .....	14
1.5    Layout of the Thesis.....	15
CHAPTER 2: LITERATURE REVIEW.....	16
CHAPTER 3: METHODOLOGY .....	20
3.1    Material Properties.....	20
<b>3.2    Details of specimens, cases investigated, and exposure Conditions.....</b>	<b>22</b>
3.2.1    Details of the specimens.....	22
3.2.2    Exposure Conditions .....	24
3.3    Method of evaluations.....	31
3.3.1    Compressive strength:.....	31
3.3.2    Macrocell corrosion: .....	31
3.3.3    Microcell corrosion:.....	32
3.3.4    Half-cell potential: .....	34
CHAPTER 4: RESULT AND ANALYSIS .....	35
4.1    Strength Test Results.....	35
4.2    Macrocell Current: .....	37

4.2.1	Macrocell Current of Case-1 .....	37
4.2.2	Macrocell Current of Case-2 .....	39
4.2.3	Macrocell Current of Case-3 .....	40
4.2.4	Macrocell Current of Case-4 .....	41
4.2.5	Macrocell Current of Case-5 .....	42
4.2.6	Macrocell Current of Case-6 .....	43
4.2.7	Macrocell Current of Case-7 .....	44
4.2.8	Macrocell Current of Cases of SC-B .....	45
4.2.9	Macrocell Current of Cases of SC-C .....	46
4.2.10	Macrocell Current of all Cases .....	47
4.3	Depth of Corrosion: .....	48
4.4	Concrete Resistance .....	49
4.5	Half-Cell Potential .....	50
4.6	Corrosion Current Density .....	51
CHAPTER 5: CONCLUSION AND RECOMMENDATION.....		53
5.1	General .....	53
5.2	Conclusion.....	53
5.3	Recommendation .....	54
REFERENCES .....		56



## List of Figures

<i>Figure 1: Research Flow Diagram</i> .....	14
<i>Figure 2: Prism specimen dimensions</i> .....	25
<i>Figure 3: Internal wire connection among the steel bars, connection to data logger and connection between the data logger and the computer.</i> .....	25
<i>Figure 4: Steel Bars cleaned with di-Ammonium hydrogen citrate</i> .....	26
<i>Figure 5: Wires Soldered to the ends of Steel Bars</i> .....	26
<i>Figure 6: Cement and Lime coated Steel Bars</i> .....	27
<i>Figure 7: Curing of Coated Steel bars</i> .....	27
<i>Figure 8: Casting of concrete specimens (placing the rebars)</i> .....	28
<i>Figure 9: Casting of concrete specimens</i> .....	28
<i>Figure 10: Curing of concrete specimens</i> .....	29
<i>Figure 11: Crack width of 0.2 mm (side view)</i> .....	29
<i>Figure 12: Crack width of 0.2 mm (top view)</i> .....	30
<i>Figure 13: Measurement of micro-cell corrosion</i> .....	33
<i>Figure 14: Measurement of micro-cell corrosion</i> .....	33
<i>Figure 15: Macrocell Current of Case-1</i> .....	37
<i>Figure 16: Macrocell Current of Case-2</i> .....	39
<i>Figure 17: Macrocell Current of Case-3</i> .....	40
<i>Figure 18: Macrocell Current of Case-4</i> .....	41
<i>Figure 19: Macrocell Current of Case-5</i> .....	42
<i>Figure 20: Macrocell Current of Case-6</i> .....	43
<i>Figure 21: Macrocell Current of Case-7</i> .....	44
<i>Figure 22: Macrocell Current of all cases of SC-B</i> .....	45
<i>Figure 23: Macrocell Current of all cases of SC-C</i> .....	46
<i>Figure 24: Macrocell Current of all cases</i> .....	47
<i>Figure 25: Depth of Corrosion</i> .....	48
<i>Figure 26: Corrosion Resistance in different cases</i> .....	49
<i>Figure 27: Half Cell Potential in different cases</i> .....	50

## List of Tables

<i>Table 1: Coarse Aggregate (Stone Chips)</i> .....	20
<i>Table 2: Fine Aggregate</i> .....	21
<i>Table 3: Composition of slag B and Slag C cements.</i> .....	21
<i>Table 4: Properties of rebar</i> .....	21
<i>Table 5: Mix design of slag cement B and slag cement C</i> .....	21
<i>Table 6: Description of the cases</i> .....	24
<i>Table 7: Cu/CuSO<sub>4</sub> half-cell potential and probability of corrosion (ASTM C876)</i> .....	34
<i>Table 8: Strength test result</i> .....	35
<i>Table 9: Microcell corrosion Current Density in Different Cases</i> .....	51

# CHAPTER 1: INTRODUCTION

## 1.1 General

Concrete is the most frequently utilized material in the world. Corrosion of steel in concrete is a major concern as it is responsible for the degradation of concrete structures. Corrosion of steel in concrete can be caused by either carbonation or chloride ingress. According to various studies and investigations, chloride-induced corrosion has been identified as one of the main reasons for deterioration of concrete in buildings exposed to the marine environment (Mohammed, Rahman, Sabbir, Hasan and Mamun, 2021). In an online article published in 2013 on the NACE International Impact called ‘Assessment of The Global Cost of Corrosion’, the global cost due to corrosion was US \$ 2.5 trillion annually. Bangladesh was listed as having the sixth-highest risk of natural disasters like cyclones among the top ten countries in the world in 2015. Due to corrosion of steel in concrete marine infrastructures and cyclone shelters were subjected to deterioration (Miyaji, Okazaki and Ochiai, 2017). In Bangladesh many mega projects, marine infrastructures, tunnels, sea ports are ongoing in the coastal regions. These infrastructures are likely subjected to corrosion and the cost would be increased due to repair and maintenance, reduction of durability and service life. To ensure the sustainability and durability of the structures, it is necessary to facilitate the ways of controlling the corrosion in reinforcement concrete structures. Thus, suitable methods need to be applied to reduce and control the extent of corrosion. Concrete surface coating, use of epoxy coated bars, use of high-performance concrete, cathodic protection (sacrificial anode, impressed current cathodic protection) and use of corrosion inhibitors are the common methods. In this study the main focus will be on controlling the macrocell and microcell corrosion of steel bars in concrete.

## 1.2 Background

Macrocell corrosion is the corrosion process of steel bars in concrete in which a local anode and a large cathode is formed. Macrocell corrosion frequently occurs in chloride induced corrosion of rebars in concrete and is responsible for very high corrosion attacks and reduction in cross-section found in different substructures and superstructures alike (Kreft, Eckstein, Junghans, Kerestan and Hagen, 2015). In Microcell corrosion, formation of microscopic cells containing anode and cathode next to each other in a continuous steel bar is seen. In a steel bar inside concrete cover a passivation film is created as a countermeasure to corrosion in concrete due to its alkaline properties (Miyaji et al, 2017). The passivation film ruptures and corrosion cells form when the chloride level surrounding the steel bars in concrete exceeds 0.4% of cement mass or 1.2 kg/m<sup>3</sup> of concrete (Schießl, 1988). Previous study shows that more chloride ingress and corrosion activity were observed in reinforced concrete using Recycled Brick Aggregate than Stone Aggregate (Cao, Su, Hibino and Goda, 2022). Lime is known to improve the intrinsic properties of concrete and provide better resistance against corrosion. The addition of lime slurry came up with positive effects in concrete properties having pozzolans. Cement-coated steel bars are also more resistant to macrocell corrosion and chloride infiltration. The effect of lime-coated rebar on macrocell corrosion, on the other hand, remains uncertain. Slag cement outperformed other cement types in terms of resistance to chloride ingress and corrosion of steel bars in concrete (Mohammed, Hamada, and Yamaji, 2019). Use of slag can improve the intrinsic properties of concrete (Quraishi, Nayak, Kumar and Kumar, 2017), can reduce anodic steel corrosion area ratios (Quraishi et al, 2017). The performance of high slag content (>60%) in cement is better for protection against such corrosion compared to other cement types. With this context, a thorough investigation on macrocell corrosion of steel bars in cracked concrete made with slag cement needs to be investigated.

Extensive research on corrosion of steel bars in concrete made with slag cement and the effect of hydrated lime slurry injection with a view to reduce the magnitude of corrosion were merely found in the literature. This study will involve the matter to see if cement and lime coated rebars in slag B cement (having slag content around 30%) show better results against slag C cement.

### **1.3 Objectives of the study**

In this study, we embark on a quest to find ways of controlling the macrocell corrosion of steel bars in cracked concrete exposed to the marine environment. The primary objectives of this study will be:

- To control the corrosion of steel bars in concrete in marine environment.
- To identify a better cement for marine environment.

## 1.4 Research Flow Diagram

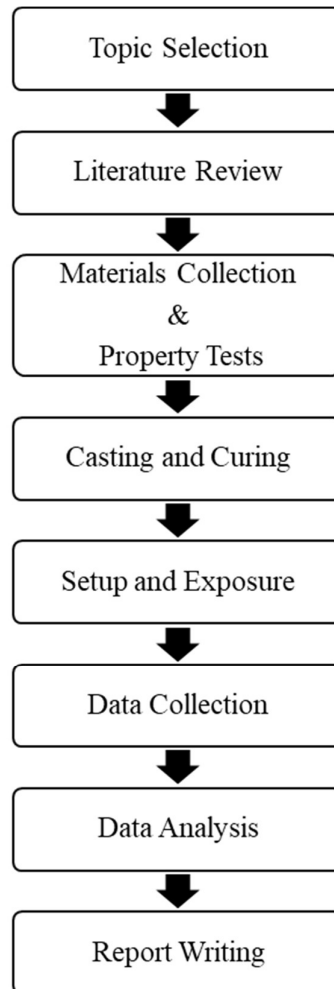


*Figure 1: Research Flow Diagram*

## **1.5 Layout of the Thesis**

The thesis consists of the following layout:

### **Chapter 1:**

Introduction - The current chapter, that discusses about the theory, background, objectives, scope of the study, research flow diagram.

### **Chapter 2:**

Literature Review - The chapter describes the related research in the field of our study by former authors and their findings.

### **Chapter 3:**

Methodology - This chapter describes the procedures and steps that were followed to conduct our study.

### **Chapter 4:**

Results and Discussion - Collected data and processing of the data, results were included in the chapter.

### **Chapter 5:**

Conclusion and Recommendations - General discussion, limitations, recommendations and future scopes of work was discussed here.

## CHAPTER 2: LITERATURE REVIEW

This chapter highlights some of the major studies and their significant findings conducted by notable researchers in the field of sustainable concrete materials. In the review paper conducted by Wang, Wang, Zhao, Li, Ji, Zou, Qiao, Zhou, Wang, Song (2023) stated that:

Based on the electrochemical mechanism of corrosion, there are several types of corrosion of reinforced concrete caused by corrosive environments. These are rebar corrosion caused by micro-corrosion cells and rebar corrosion caused by macro-corrosion cells. When comparing the two forms of corrosion, macrocell corrosion of rebar is more detrimental and has a faster corrosion rate. In the macrocell corrosion system, the cathodic rebar is protected, whilst the anodic rebar works as the corrosion carrier, becoming the principal corrosion occurrence region and sacrificial electrode. Furthermore, rebar macrocell corrosion is typically followed by microcell corrosion, further complicating the appearance of rebar corrosion. (p. 02)

Wang et. Al (2023) further listed different inducements for macrocell corrosion of rebar such as coupling of dissimilar rebars, concertation difference of service environment, ambient temperature field, difference in the areas of cathode and anode, difference in the exposure area, etc. Mohammed, Raghavan, Knight and Murugesan (2014) conducted an investigation on the corrosion resistance of steel rebars with multiple coatings, such as cement-polymer composite coatings with a preset damage area of 1%, cement slurry inhibiting coatings, zinc plating coatings, and cement-polymer anti-corrosion coating and they came to the conclusion that a small amount of coating damage did not bear great significance on the macrocell corrosion of rebars. The field of macrocell corrosion is of utmost importance. However, the number of relevant research being done is abysmal.

There are many researchers who provided outlines on how to better prepare for this challenge. Wang et al (2023) summarized the procedure that will ensure the comprehensive protection of reinforced concrete structures (RCS) throughout design, material selection, construction, management, and maintenance, significantly improving their durability and service life in demanding environments. This entails developing high-performance rebars with superior corrosion resistance and economic viability, optimizing design and construction schemes for minimal macrocell corrosion risk, implementing accurate monitoring techniques for damage assessment and residual life prediction, and adopting integrated technologies for repair of



corrosion damage and improvement of durability. However, with the goal of sustainable development many of these procedures need to be further discussed and analyzed.

Mohammed and Hamada (2006) undertook a comprehensive investigation to analyze the corrosion of steel bars and steel-concrete interfaces in concrete specimens with varying surface conditions of steel bars: mill-scaled, polished, brown-rusted, black-rusted, and pre-passivated. The ascending sequence of chloride threshold levels over the steel bars is mill-scaled, brown-rusted, black-rusted, polished and pre-passivated. Additionally, when a cement paste coating was applied to rebar, it resulted in a substantially denser steel-concrete interface compared to the other investigated cases, greatly improving the chloride threshold level.

Mohammed, Hamada, Manum, A. and Hasnat (2013) conducted a detailed experimental investigation to assess the effectiveness of cement paste coated steel bars in preventing chloride-induced corrosion. Concrete specimens with embedded steel bars were subjected to accelerated cycles of chloride exposure. Results showed that with the application of .25 mm thick cement paste coating the time to initiate corrosion was significantly extended for coated steel bars, especially with lower water-to-cement ratios. Determining the chloride threshold for the initiation of corrosion required careful consideration of the characteristics of the steel-concrete contact. Additionally, a proposed relationship between water soluble and acid soluble chloride content in concrete was introduced (Mohammed et al, 2013).

Mohammed et al, (2021) conducted a study on the corrosion of steel bars caused by macro-cell corrosion and chloride ingress in concrete built using recycled brick aggregate (RBA). They used virgin stone aggregate (SA) and brick aggregate (BA) as control cases. Half-cell potential, corrosion area, and pit depth or corrosion depth were evaluated. The order of macrocell current density and corrosion depth in respect to aggregate type is RBA > BA > SA. In short, stone aggregate performs better against corrosion. Lins, Michele & Costa, Cintia & Araujo and Carlos (2019) conducted a study with the goal to find out how lime in cement mortar influences the corrosion resistance of carbon and galvanized steel reinforcements. After 36 months of cycle testing with three different lime concentrations (6.7, 13.3, and 26.3 wt.%) they found that the polarization resistance of rebar in mixed mortars with the highest lime concentration was the lowest.

Valcuende, Calabuig, Martinez-Ibernón, and Soto (2020) studied the influence of finely ground hydrated lime on chloride-induced reinforcement corrosion in eco-efficient concrete made with 50% cement replacement by fly ash and various lime percentages (0%, 10%, and 20%). Six

tests were performed. They included chloride migration, rapid chloride migration, and corrosion rate. They discovered that the pozzolanic interaction between fly ash and lime resulted in enhanced density of the cementitious matrix. This results in improved electrical resistance and a decreased corrosion rate. Chloride penetration is substantially lower in concretes containing 50% cement replaced by fly ash and a maximum of 20% lime than in concretes containing no fly ash or lime (Valcuende et al., 2020).

Using the macrocell corrosion theory and alternating the microcell corrosion state and macrocell corrosion state, the influence of mineral admixtures such as fly ash, slag, and limestone powder on the macrocell corrosion behaviors of steel bars embedded in chloride-contaminated concrete was investigated and clarified by Cao et al, (2022). Cao et al. (2022) came to the conclusion that Slag prevented macrocell and microcell corrosion more effectively than fly ash or limestone powder. Furthermore, when 70% slag replaced cement, concrete contaminated by chloride showed lower anodic steel corrosion area ratios. They reached the conclusion that usage of slag and fly ash in chloride-contaminated concrete can significantly reduce macrocell corrosion while favoring microcell corrosion.

The marine durability of 30-year-old concrete specimens, manufactured using different cement types (ordinary Portland cement, high early strength Portland cement, moderate heat Portland cement, slag cement type B, and alumina cement), was examined Mohammed, Hamada and Yamaji (2003). Parameters such as sulfate content, mixing water, and exposure zones were considered. Evaluations encompassed compressive strength, chloride ingress, corrosion of steel bars, microstructure, mineralogy, and interfaces. Chloride ingress followed the sequence OPC, HES, MH, SCB and AL. Because of chloride and ion penetration from saltwater, SCB and AL had decreased pore volume at the outer area. (Mohammed et al, 2003).

Mohammed et al, (2019) experimented with a view to finding out the durability of concrete in seawater. To verify the long-term durability of concrete incorporating slag cement in seawater, a group of three concrete specimens were examined after 10, 15, and 30 years of exposure to marine tides. Physical appearance, mineralogy, chloride intrusion, carbonation depth, compressive strength, concrete resistivity, microstructures, rebar corrosion, and concrete interfaces were all assessed. Slag cement outperformed conventional Portland cement (OPC) in terms of long-term strength improvement. After extended marine exposure, the microstructure of slag cement concrete at the surface densified, effectively limiting chloride

penetration. Slag cement demonstrated superior resistance to chloride ingress and corrosion of steel bars in concrete.

Lime addition is known to improve the intrinsic properties of concrete and provide better resistance against corrosion. Mira, Papadakis and Tsimas (2002) discovered that the inclusion of lime slurry had a good influence on the qualities of pozzolan-containing concrete and a slightly negative effect on the properties of pure Portland cement. Cement coated steel bars also provide better protection against macrocell corrosion and chloride ingress. However, the effect of lime coated rebar in macrocell corrosion is unknown. When compared to other cement kinds, cement with a high slag concentration (>60%) performs better in terms of corrosion resistance. Will cement and lime coated rebar in slag B cement (slag percentage of roughly 30%) outperform slag C cement? This is the core focus of our research.

## CHAPTER 3: METHODOLOGY

### 3.1 Material Properties

Coarse aggregate that was used for this experiment was stone chips (SC). The size distribution was maintained as per ASTM C33. Specific gravity and absorption capacity was 2.66 and 0.9 respectively following the specification ASTM C127. Specific gravity and fineness modulus for fine aggregate was 2.68 and 2.44 respectively while following the specification ASTM C127 and ASTM C136 respectively. The properties of coarse and fine aggregate are summarized in table-1 and table-2. Two different types of cement were used for this research. 'Slag cement B', 32% slag content, and 'slag cement C', 70% slag content, were used. The summary of the cement properties can be viewed in table-3. For the research, steel bars of 10 mm diameter Grade 500W (manufactured in accordance with ASTM A706, minimum yield strength = 500 MPa) were employed. Table-4 summarizes the chemical compositions of rebar.

*Table 1: Coarse Aggregate (Stone Chips)*

Tests	Specification	Result
Specific Gravity	ASTM C127	2.66
Absorption Capacity (%)	ASTM C127	0.9
Abrasion Value (%)	ASTM C131	26.8
Unit weight (kg/m <sup>3</sup> )	ASTM C29	1978

Table 2: Fine Aggregate

Tests	Specification	Result
Specific Gravity	ASTM C127	2.68
Absorption Capacity (%)	ASTM C127	2.67
Fineness Modulus	ASTM C136	2.44
Unit weight (kg/m <sup>3</sup> )	ASTM C29	1502

Table 3: Composition of slag B and Slag C cements.

Types	Clinker (%)	Slag (%)	Gypsum (%)
SC-B	65	32	3
SC-C	28	70	2

Table 4: Properties of rebar

Element	Fe	C	Mn	Si	Si	P
Percentage (%)	98.868	0.22	0.65	0.2	0.031	0.031

Table 5: Mix design of slag cement B and slag cement C

Cement	W/C	Cement	Water (kg/m <sup>3</sup> )	Fine Aggregate	Coarse Aggregate
		(kg/m <sup>3</sup> )		(kg/m <sup>3</sup> )	(kg/m <sup>3</sup> )
SC-B	0.45	340	153	838	1060
SC-C	0.45	340	153	836	1058

## **3.2 Details of specimens, cases investigated, and exposure Conditions**

### **3.2.1 Details of the specimens**

Seven different cases were investigated for this experiment and a total of 12 prism specimens (400 mm x 100 mm x 100 mm) were created for the cases. Furthermore, twenty-four-cylindrical (200mm x 100mm) specimens were also created for strength testing. The mix design for the concrete specimens were made using Slag cement B and slag cement C. The design is based on weight-based mix design. For both designs a water to cement ratio of .45 was maintained. Cement contents were 340 kg/m<sup>3</sup>. Potable tap water was used as the mixing water for concrete. The mix design is summarized in table-5. In each prismatic specimen two steel bars are placed. One is a continuous steel bar whereas the other one is a segmented one. The purpose of the continuous one is to prevent the collapse of the specimen during cracking and that of the segmented one is to measure macrocell corrosion current among the rebars at cracked and un-cracked regions. The steel bars were first cleaned using 10% di-Ammonium hydrogen citrate solution as shown in figure-4. The length of the continuous segment is 340 mm. The segmented rebars have three parts. Two 135 mm length steel bars have a 50 mm rebar in between. The sides of the 50 mm rebar are connected to one side of the 135 mm ones with epoxy. A hole of 2.5 mm in diameter and around 5 mm in length is drilled into every steel bar along the center of their sides to insert wires. The holes and the wires are connected by soldering as shown in figure-6. The epoxy effectively shuts down the hole so that any type of fluid is barred entry into the hole. There were also two specimens which had coated steel bars. One was coated in .25mm thick cement paste having 0.5 w/c ratio whereas the other one was coated (.25 mm thick) in lime slurry containing 0.5 water to lime ratio (figure-6). The coated steel bars were cured for 24 hours (figure-7) This enabled the use of a 100  $\Omega$  resistor at each gap between

segments and in series with the segments to detect voltage loss. A data logger (TDS 150) was used to record the voltage decreases at predefined intervals. The cover concrete was 20 mm thick. The dimensions and layout of the steel bars in the specimen is shown in figure-2. Wire connection among the steel bars and connection to the data logger are shown in figure-3.

After casting (figure-8 and figure-9) the prismatic specimens were cured for 28 days in jute bags which were tightly wrapped in polythene to prevent the escape of moisture (figure-10). A notch (3mm in width and 10mm in depth) was made at the bottom face of the specimen to ensure the crack location as shown in figure-11 and figure-12. The crack on the specimens were made manually. The specimens were anchored with a very thick steel plate in support with a roller at the middle. Tightening the clamps increased the bending moment and caused micro cracks to form at the notch. The target was to keep a controlled crack width of 0.2 mm across all the specimens. After anchoring the specimens were connected to the data logger and then initially submerged in seawater collected from the Bay of Bengal.

### 3.2.2 Exposure Conditions

For this experiment we had two different types of exposure conditions. These are mentioned below:

1) Submerged in sea water for 30 days.

2) 5 cycles of;

2 days Submerged in sea water,

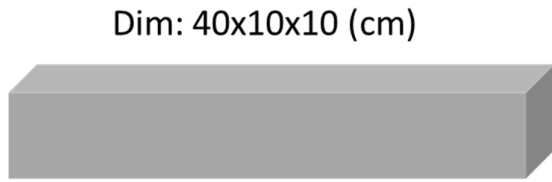
2 days in dry condition,

#### Description of the Cases

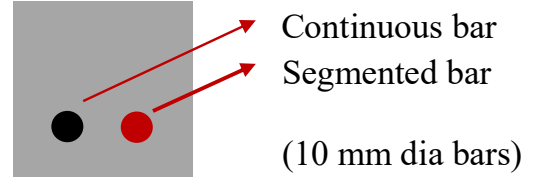
*Table 6: Description of the cases*

Case	Cement	Steel	Treatment	Details
Case 1	SC-B	Normal	Untreated	Control Case
Case 2	SC-B	Normal	Treated with Lime Slurry	Lime Slurry injected before Submerging
Case 3	SC-B	Normal	Treated with Lime Slurry	Lime Slurry injected after 3 days of submerging.
Case 4	SC-C	Normal	Untreated	Control Case
Case 5	SC-C	Normal	Treated with Lime Slurry	Treated with Lime Slurry
Case 6	SC-B	Lime Coated	Treated with Lime Slurry	Lime Slurry injected before Submerging
Case 7	SC-B	Cement Coated	Treated with Lime Slurry	Lime Slurry injected before Submerging





Specimen Dimensions



Cross sectional view of prism specimen

Figure 2: Prism specimen dimensions

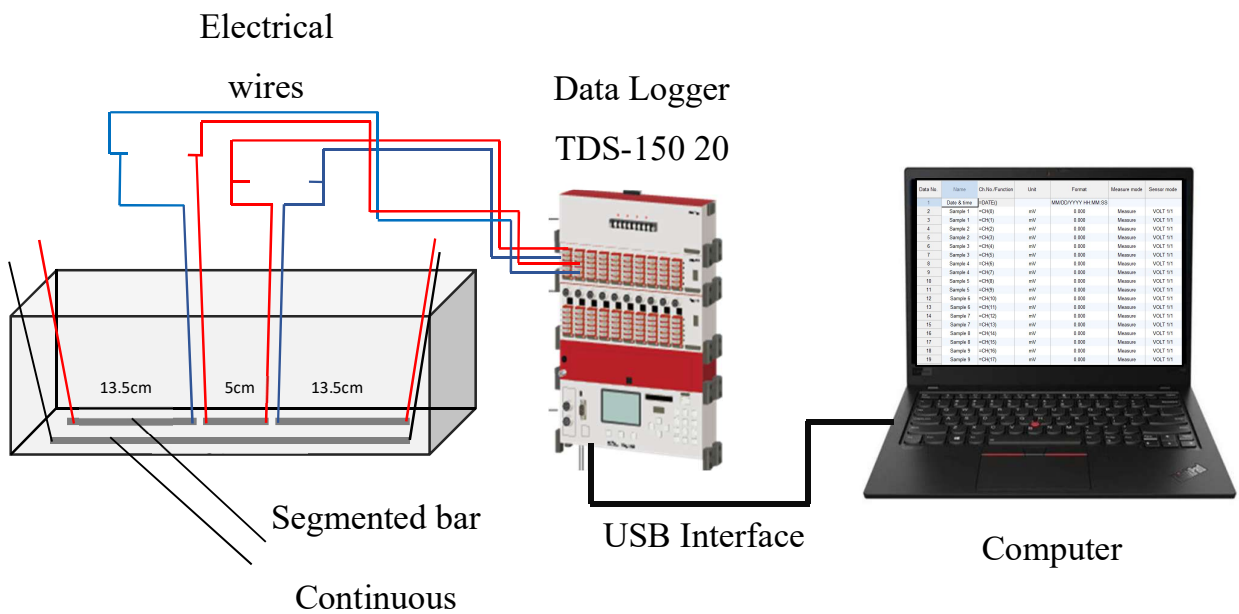
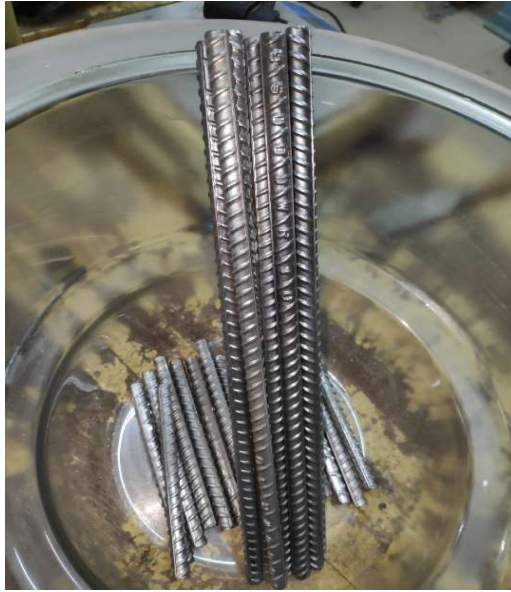
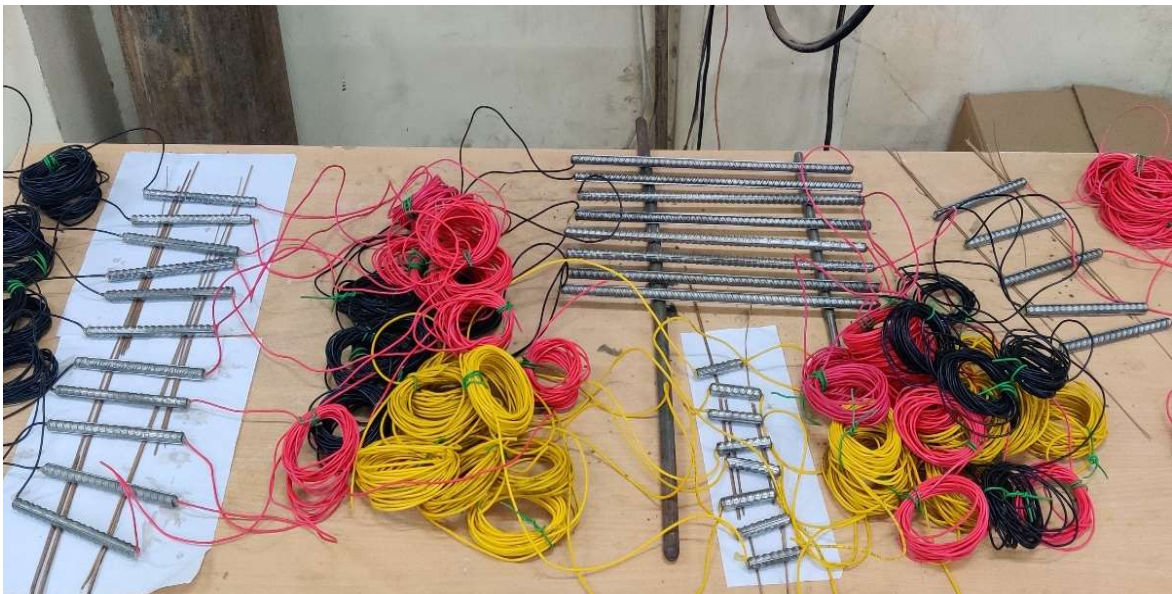


Figure 3: Internal wire connection among the steel bars, connection to data logger and connection between the data logger and the computer.



*Figure 4: Steel Bars cleaned with di-Ammonium hydrogen citrate*



*Figure 5: Wires Soldered to the ends of Steel Bars*

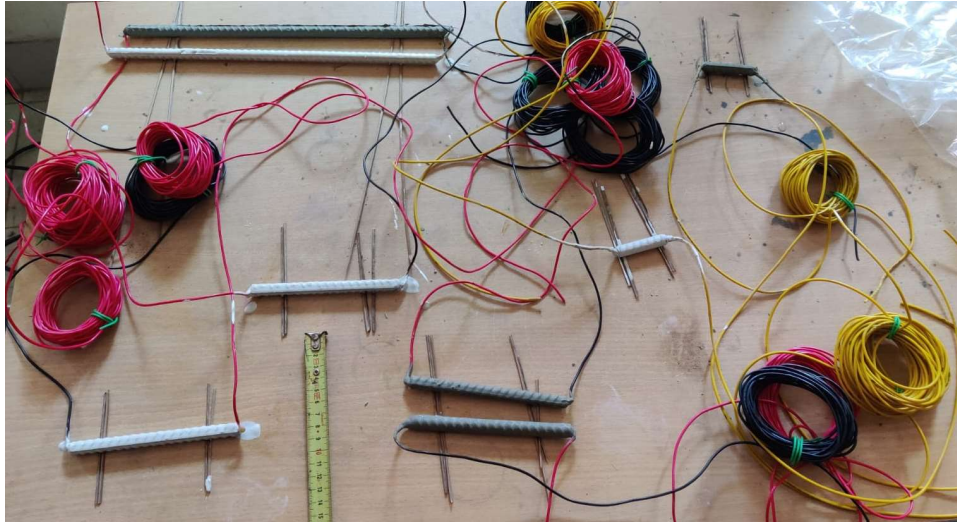


*Figure 6: Cement and Lime coated Steel Bars*



*Figure 7: Curing of Coated Steel bars*



*Figure 8: Casting of concrete specimens (placing the rebars)*



*Figure 9: Casting of concrete specimens*



Figure 10: Curing of concrete specimens

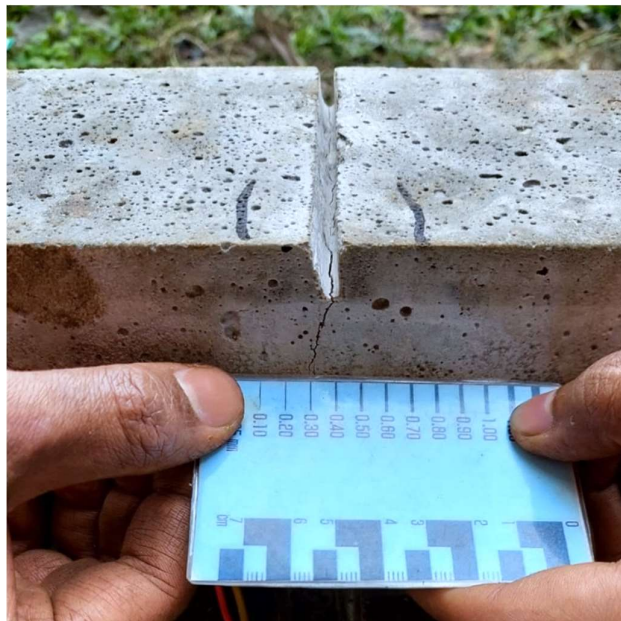


Figure 11: Crack width of 0.2 mm (side view)



*Figure 12: Crack width of 0.2 mm (top view)*

### **3.3 Method of evaluations**

#### **3.3.1 Compressive strength:**

Cylindrical specimens (100 mm in diameter and 200 mm in length) were made to conduct the compressive strength test as per ASTM C39.

#### **3.3.2 Macrocell corrosion:**

Macrocell corrosion is an electrochemical process in which the passivating layer of steel is lost (Quraishi M. A. et al, 2017). The macro-cell corrosion was measured using a data logger (TDS 150). A 100  $\Omega$  resistance was put external to the samples but in series with the steel segments to assess voltage loss owing to current between anode (cracked segment) and cathode (un-cracked segment). A crack was made along the center of the specimen. This allowed the central segment of the steel to act as anode and the un-cracked segments to act as cathode. The voltage drops were recorded for both the exposure conditions at pre-fixed time intervals. For the first 2 hours of the experiment voltage drop of every second was recorded after that for the entire duration of the experiment voltage drop after every 60 seconds was recorded. A figure showing the data logger setup is presented in figure-4. The current flow from the measured voltage drop via a fixed resistance of 100  $\Omega$  was calculated using the equation below:

$$I = \frac{V}{R}$$

Here,  $I$  is current (in ampere),  $V$  is the voltage drop and  $R$  is resistance (100  $\Omega$ )

Macrocell current density was measured using the following equation:

$$I_{mac} = \frac{I}{A} \times 10^6$$

Here,  $I_{mac}$  denotes the macro-cell corrosion current density,  $I$  denote the current and  $A$  represents the steel surface area in  $\text{cm}^2$ .

The voltage measurement system was checked if calibration id needed or not by-passing known currents of 1, 2, 3  $\mu\text{A}$  through the 100  $\Omega$  resistance and measuring the voltage drops (98, 197 and 298  $\mu\text{V}$  respectively) that were received using the device. This indicated that the experimental setup is capable of measuring the current flow with almost 98.4% accuracy.

The equation used to measure the depth of corrosion over the rebar is as follows:

$$D = 0.0016 \times I_{mac} \times t \text{ (Gonzalez et al, 1995)}$$

where  $D$  denotes corrosion depth in mm,  $I_{mac}$  denotes macro-cell corrosion current density in  $\mu\text{A}/\text{cm}^2$ , and  $t$  denotes time in years.

### **3.3.3 Microcell corrosion:**

Microcell corrosion was measured before and after the exposure condition using the ‘corro-map’ device as shown in figure-13 and figure-14.





Figure 13: Measurement of micro-cell corrosion

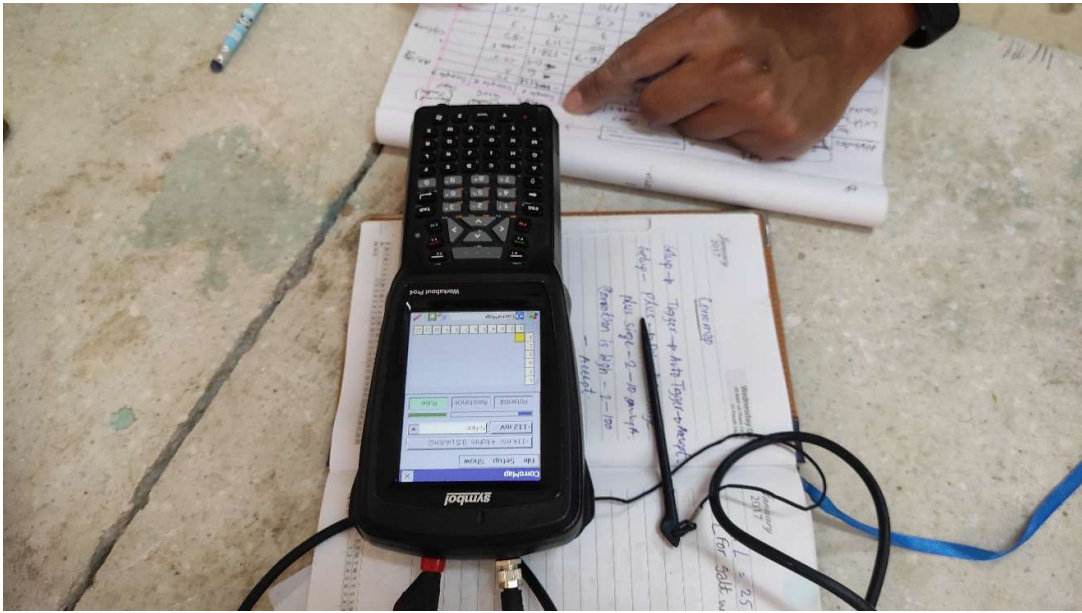


Figure 14: Measurement of micro-cell corrosion

### 3.3.4 Half-cell potential:

Cu/CuSO<sub>4</sub> half-cell was used to determine the half-cell potential before and after the introducing the exposure conditions. After measuring the macro-cell corrosion current continuously for 30 days, the half-cell potentials were measured over the segmented steel bars. This was done to avoid any disruptions in the flow of macro-cell corrosion current. To guarantee reliable readings, a single piece of steel was electrically separated from the others while measuring its potential. The probability of different half-cell potential (Cu/CuSO<sub>4</sub>) values were determined as per ASTM C876 as mentioned in table-7.

*Table 7: Cu/CuSO<sub>4</sub> half-cell potential and probability of corrosion (ASTM C876)*

Half-cell potential reading (mV)	Corrosion probability (%)
Greater than -200 mV	90% probability of no corrosion
Between -200 mV to -350 mV	Immediate corrosion risk
Less than -350 mV	90% probability of corrosion

# CHAPTER 4: RESULT AND ANALYSIS

## 4.1 Strength Test Results

Table 8: Strength test result

Cement Type	Time (Days)	Avg Strength (MPa)
SC-B	3	18.39
	28	27.65
SC-C	3	16.92
	28	25.45

According to the ASTM (American Society for Testing and Materials) testing protocol, Slag Cement Type-B (SC-B) and Slag Cement Type-C (SC-C) are two distinct types of slag cement that were used in concrete samples shown in Table 1. The findings show that both at 3 days and 28 days after curing, concrete specimens made with SC-B showed greater strength than those made with SC-C.

The increased proportion of clinker contained in this kind of slag cement can be responsible for the SC-B concrete's improved strength performance. Concrete's binding characteristics are provided by clinker, an essential ingredient in the manufacture of cement. Greater clinker levels in SC-B cement results in a more effective hydration process and improved production of calcium silicate hydrates, which are in responsible for giving concrete its strength.

The findings of the 3-day strength test show that both SC-B and SC-C concrete gained strength quickly. But even at this young age, the SC-B concrete showed a significant strength advantage

over the SC-C concrete. This demonstrates the faster pozzolanic reaction and the advantageous effect of SC-B's greater clinker concentration.

Additionally, the 28-day strength results emphasize the continuing strength growth of SC-B concrete and support the findings seen at 3 days. This demonstrates the faster pozzolanic reaction and the advantageous effect of SC-B's greater clinker concentration. The 28-day strength results emphasize the continued strength growth of SC-B concrete and support the findings seen at 3 days.

## 4.2 Macrocell Current:

### 4.2.1 Macrocell Current of Case-1

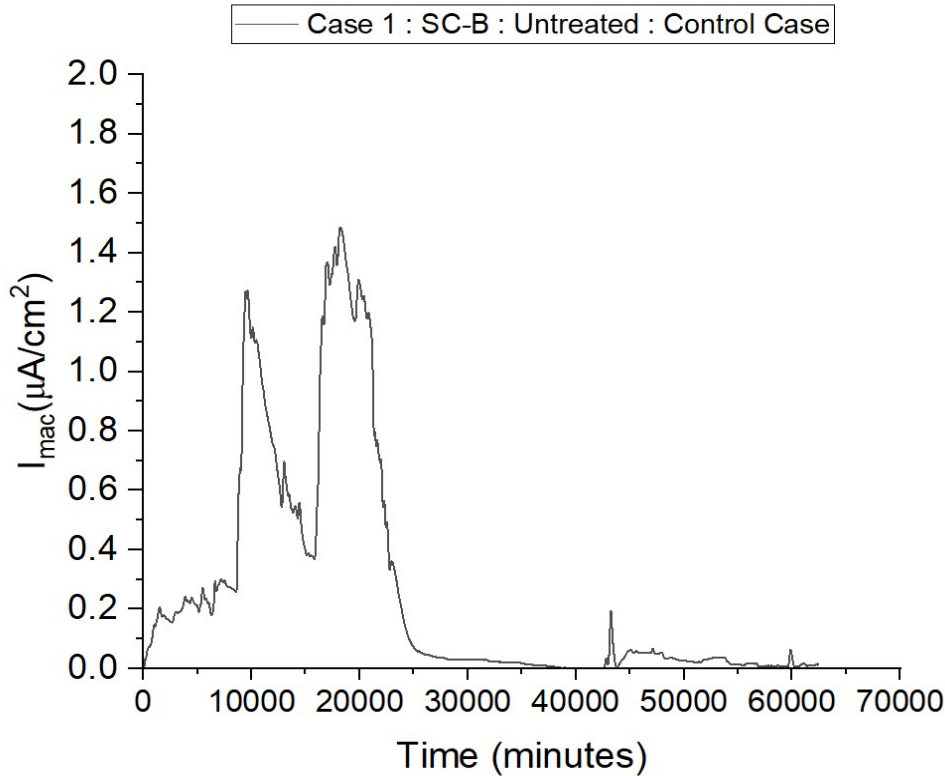


Figure 15: Macrocell Current of Case-1

illustrates the macrocell current versus exposure time graph for Case-1, which serves as the control case in the study. In this case, Slag Cement Type-B (SC-B) was utilized without any additional treatment. Slag Cement Type-B (SC-B) was used in this case without any extra treatment. The figure shows the macrocell current over a period of 62,351 minutes in a graphical manner.

When the graph is evaluated, it becomes evident Case-1's mean macrocell current value is  $0.2561057 \mu A/cm^2$ . Initially, the current density was very higher, but after a period of time the current density was declining and lastly it became a stable value. A concrete and

reinforcement's electrochemical activity, which is mainly driven by the presence of various materials, moisture, and possible chemical reactions, is measured by the macrocell current.

The average value of macrocell current provides information about the concrete sample's electrochemical activity. It shows the average strength of the macrocell current that has been seen passing through the concrete throughout the time period under observation.

The macrocell current's results from its capacity to reveal a sign of corrosion activity within the rebar. Higher macrocell currents are frequently linked to higher rates of corrosion, which raises the possibility that the steel reinforcing bars or other metal components contained in the concrete may corrode.

The measured mean macrocell current value of  $0.2561057 \mu\text{A}/\text{cm}^2$  in Case-1, when SC-B was utilized without any treatment, indicates some electrochemical activity. To assess the concrete's corrosion susceptibility or protective behavior in this particular situation, comparisons with other cases or control groups are investigated.

## 4.2.2 Macrocell Current of Case-2

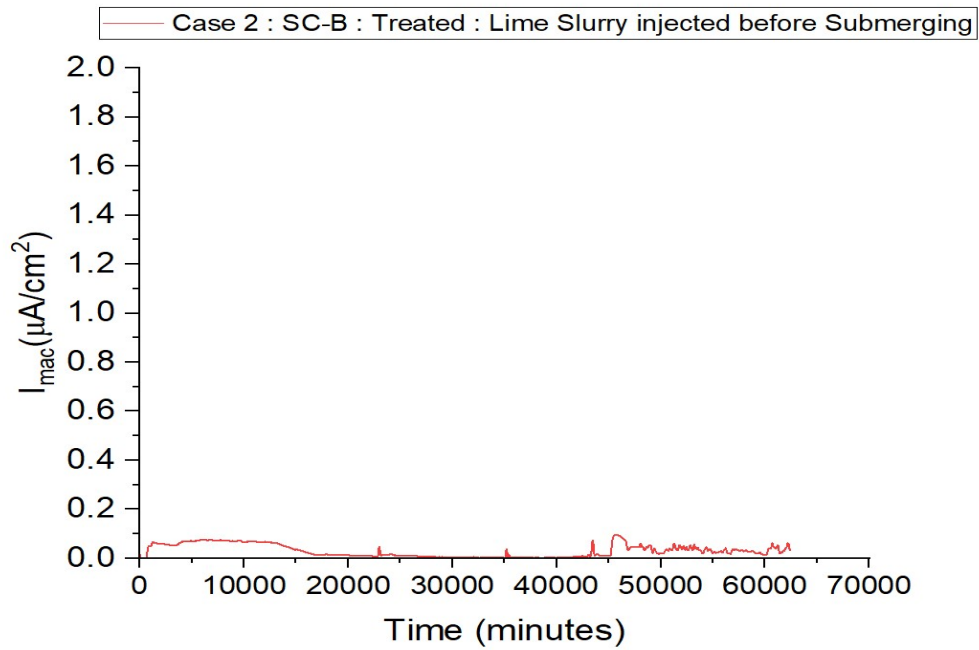


Figure 16: Macrocell Current of Case-2

The macrocell current versus time of exposure graph for Case-2 is shown in Fig-2. It is the case using SC-B and lime slurry treatment before submerging in seawater. As the treatment was done before submerging in seawater, the rapid increase of corrosion was absent here. The mean value of macrocell current is  $0.0298186 \mu\text{A}/\text{cm}^2$ .

### 4.2.3 Macrocell Current of Case-3

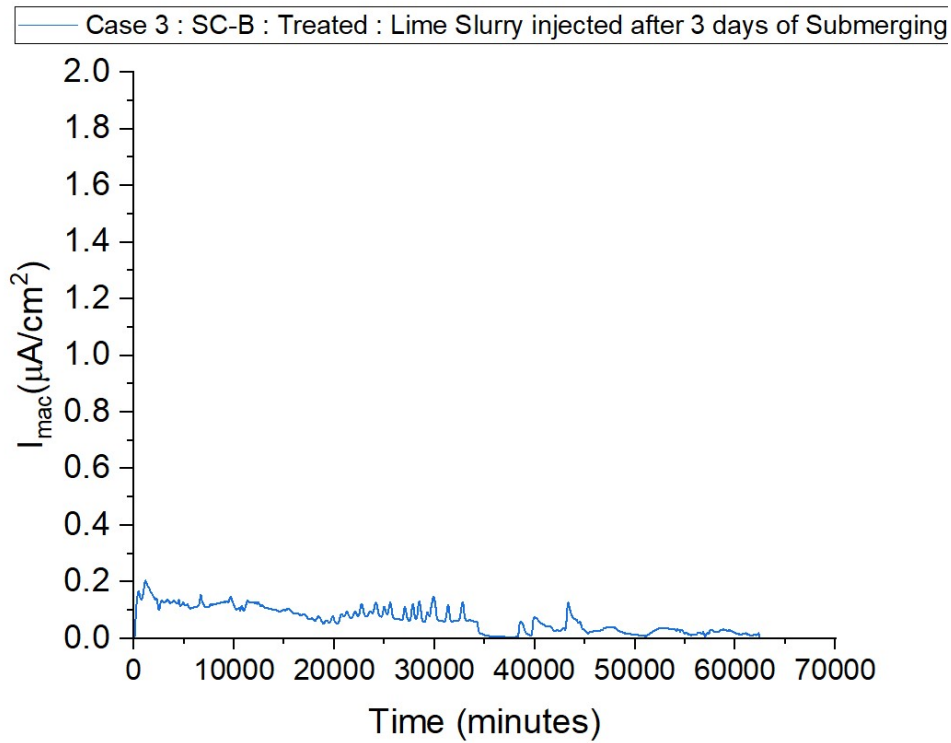


Figure 17: Macrocell Current of Case-3

The macrocell current versus time of exposure graph for Case-3 is shown in Fig-3. It is the case using SC-B and lime slurry treatment after 3 days of submerging in seawater. Before the treatment was done, there is a rapid increase of corrosion current density. After the treatment was done, the corrosion current density was declining. The mean value of macrocell current is  $0.0672844 \mu\text{A}/\text{cm}^2$ .



#### 4.2.4 Macrocell Current of Case-4

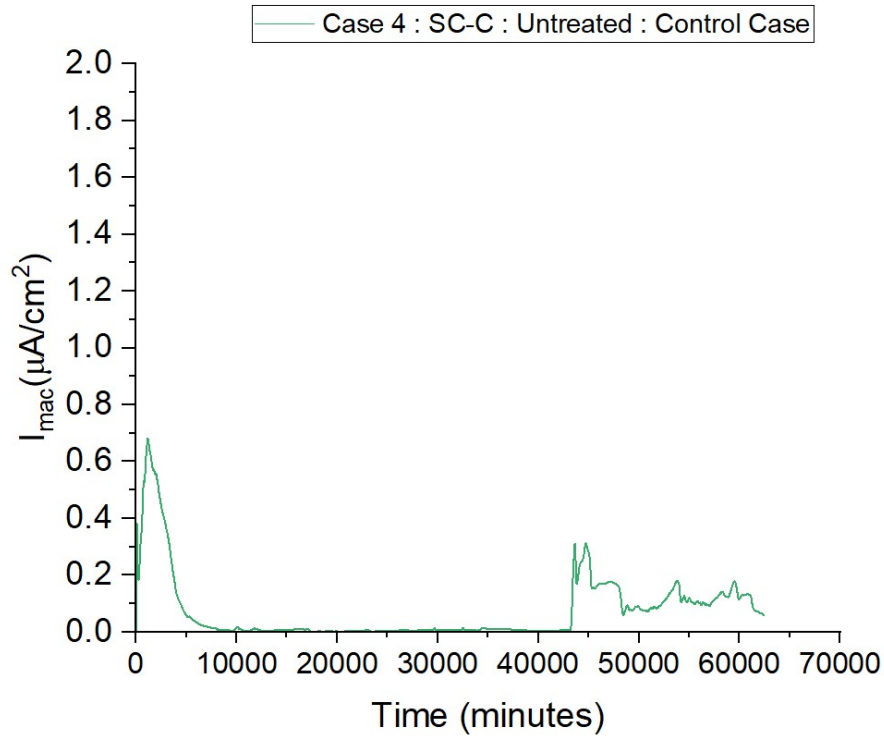


Figure 18: Macrocell Current of Case-4

The macrocell current versus time of exposure graph for Case-4 is shown in Fig-4. It is the case using SC-C and no treatment. When the graph is evaluated, it becomes evident Case-4's mean macrocell current density value is  $0.0734713 \mu A/cm^2$ . Initially, the current density was very higher, but after a period of time the current density was declining and lastly it became a stable value.

#### 4.2.5 Macrocell Current of Case-5

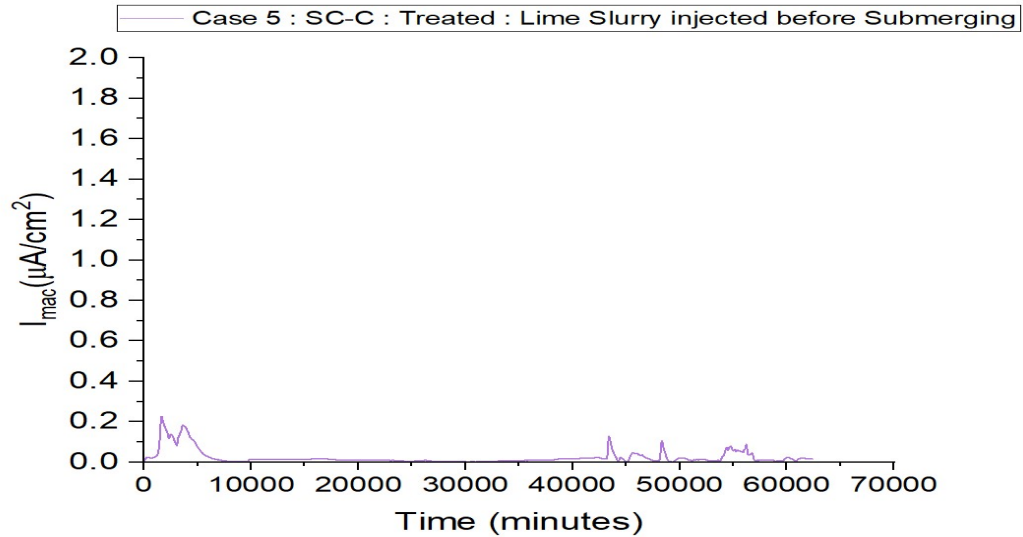


Figure 19: Macrocell Current of Case-5

The macrocell current versus time of exposure graph for Case-5 is shown in Fig-5. It is the case using SC-C and lime slurry treatment before submerging in seawater. Initially the corrosion current density was higher as submerging in seawater caused a rapid increase of the values. After a period of time, the values were declining, then became stable. The mean value of macrocell current is 0.0232282  $\mu A/cm^2$ .

#### 4.2.6 Macrocell Current of Case-6

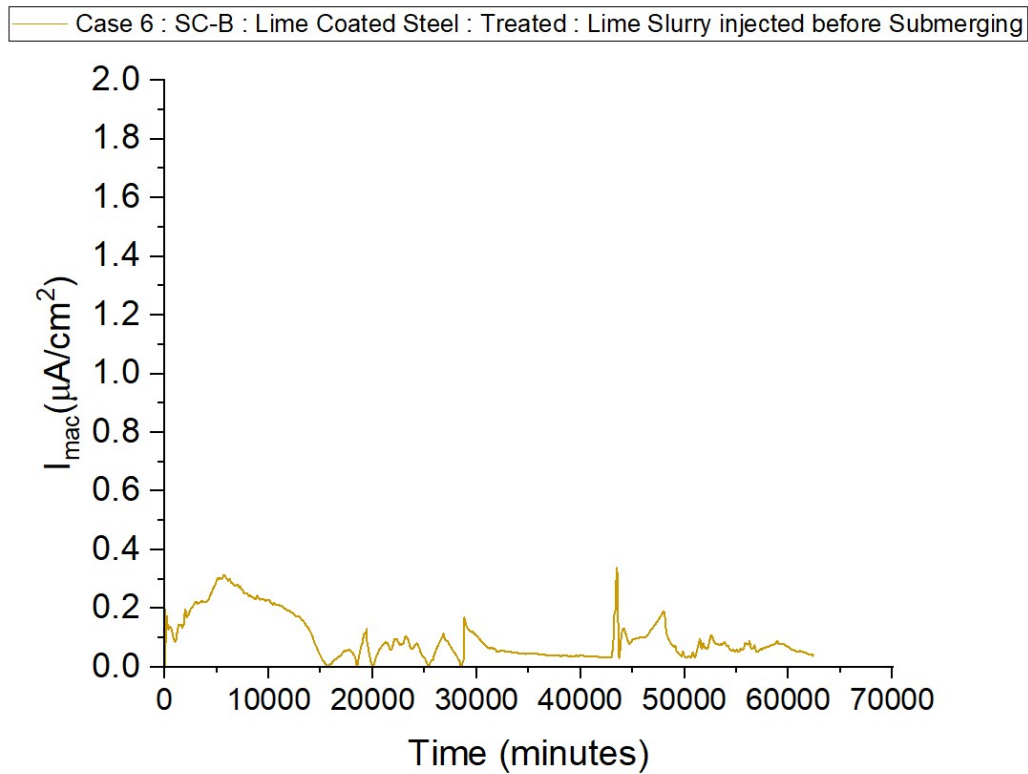


Figure 20: Macrocell Current of Case-6

The macrocell current versus time of exposure graph for Case-6 is shown in Fig-6. It is the case using SC-B, lime-coated steel bar and lime slurry treatment before submerging in seawater. Initially, there is a rapid increase in corrosion current density. After some time, the corrosion current density was declining. The mean value of macrocell current is  $0.0989368 \mu A/cm^2$

#### 4.2.7 Macrocell Current of Case-7

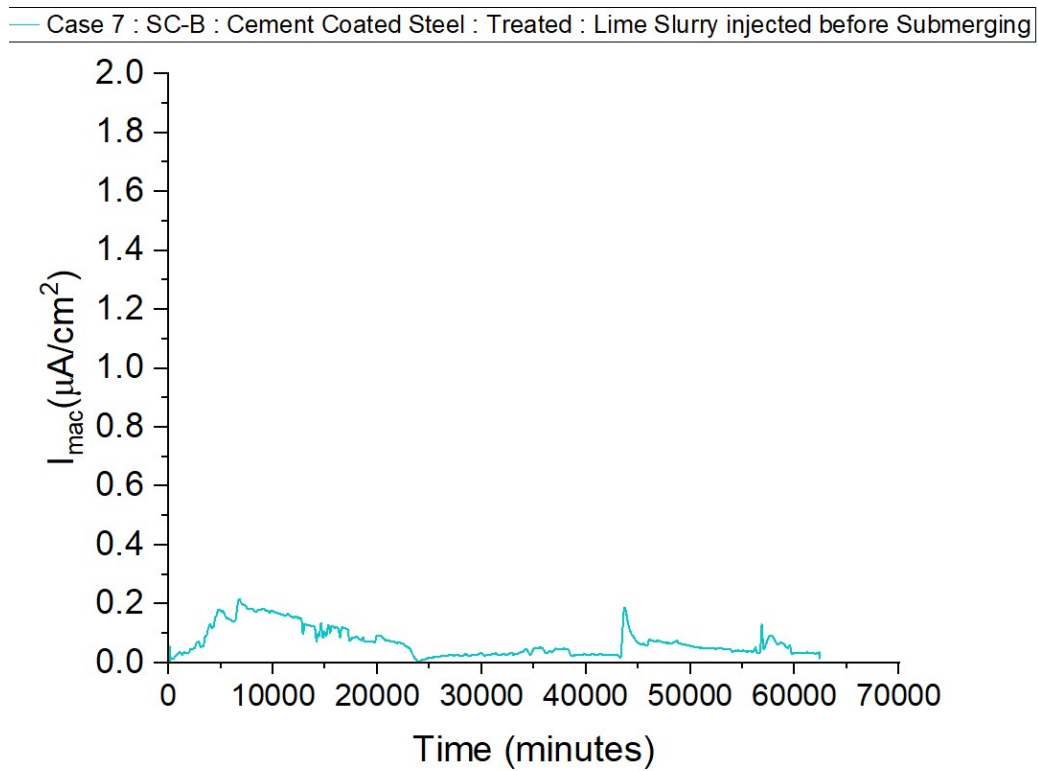


Figure 21: Macrocell Current of Case-7

The macrocell current versus time of exposure graph for Case-7 is shown in Fig-7. It is the case using SC-B, cement-coated steel bar, and lime slurry treatment before submerging in seawater. Initially, there is a rapid increase in corrosion current density. After some time, the corrosion current density was declining. The mean value of macrocell current is  $0.0695883 \mu A/cm^2$

## 4.2.8 Macrocell Current of Cases of SC-B

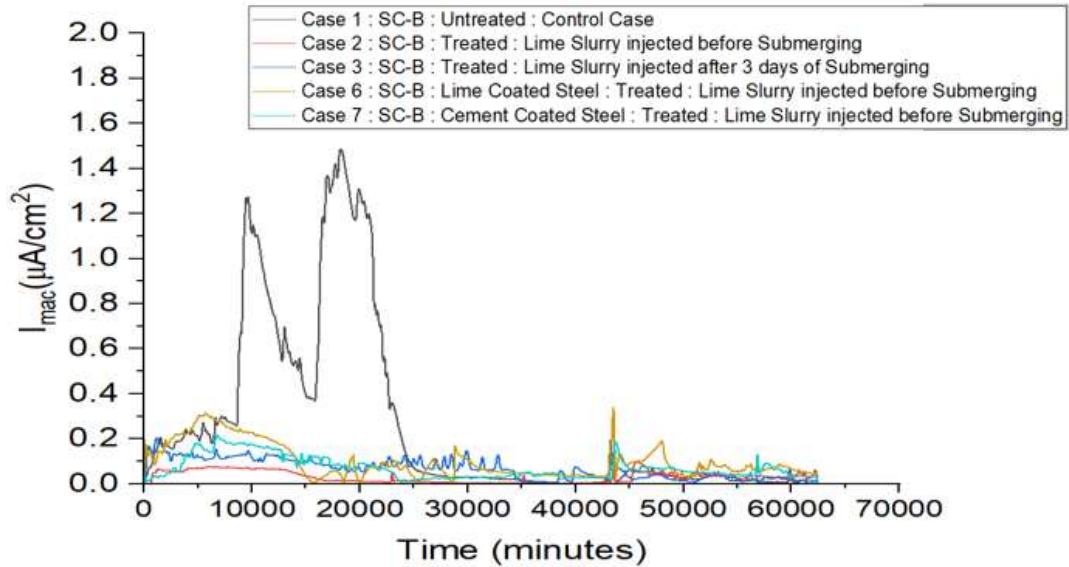


Figure 22: Macrocell Current of all cases of SC-B

The macrocell current versus time of exposure graph for Cases using SC-B is shown in Fig-8. The cases are Case 1, Case 2, Case 3, Case 6, Case 7. Analyzing the graph, we can conclude that the most effective treatment process is used in Case 6. Then case 7, Case 2 and case 3 respectively. Using lime coated steel bar and injecting lime slurry injected before submerging in seawater is the best solution for SC-B.

## 4.2.9 Macrocell Current of Cases of SC-C

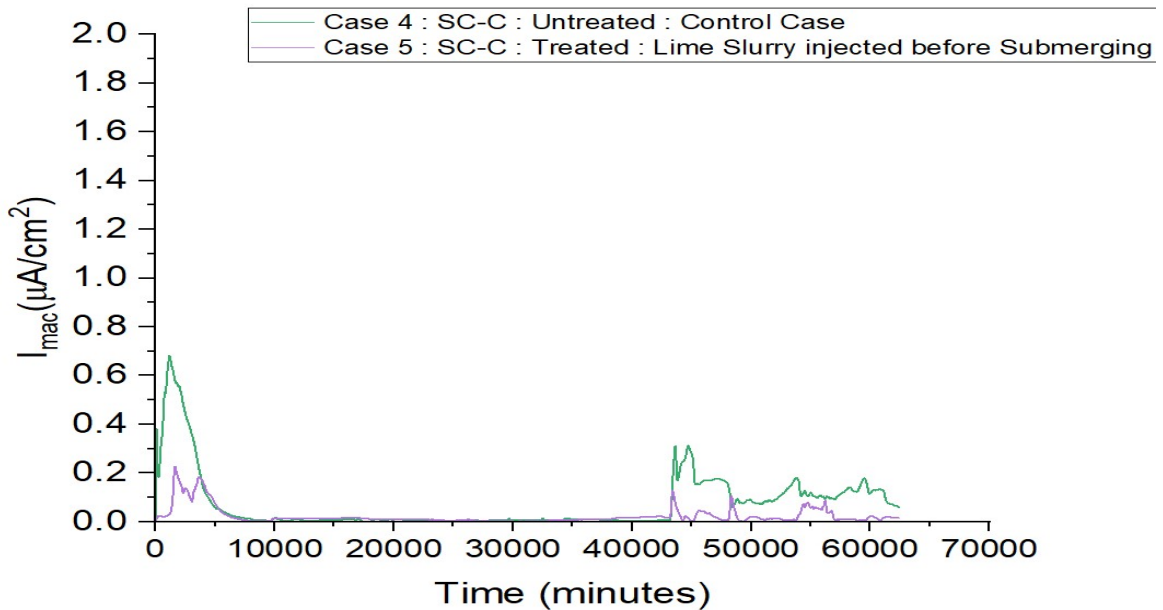


Figure 23: Macrocell Current of all cases of SC-C

The macrocell current versus time of exposure graph for Cases using SC-C is shown in Fig-9. The cases are Case 4 and Case 5. Analyzing the graph, we can conclude that the corrosion current density in both cases is very low as there is more slag content in these cases. Slag has pozzolanic properties, meaning it can react with calcium hydroxide and contribute to the formation of additional calcium silicate hydrates (C-S-H) gel. This reaction leads to increased hydration, resulting in a denser and more impermeable concrete matrix. By reducing the permeability of concrete, slag helps to limit the movement of aggressive agents, such as chlorides and sulfates, which are the primary culprits in causing corrosion. After treatment with lime slurry in Case 5, the macrocell current has reduced.

#### 4.2.10 Macrocell Current of all Cases

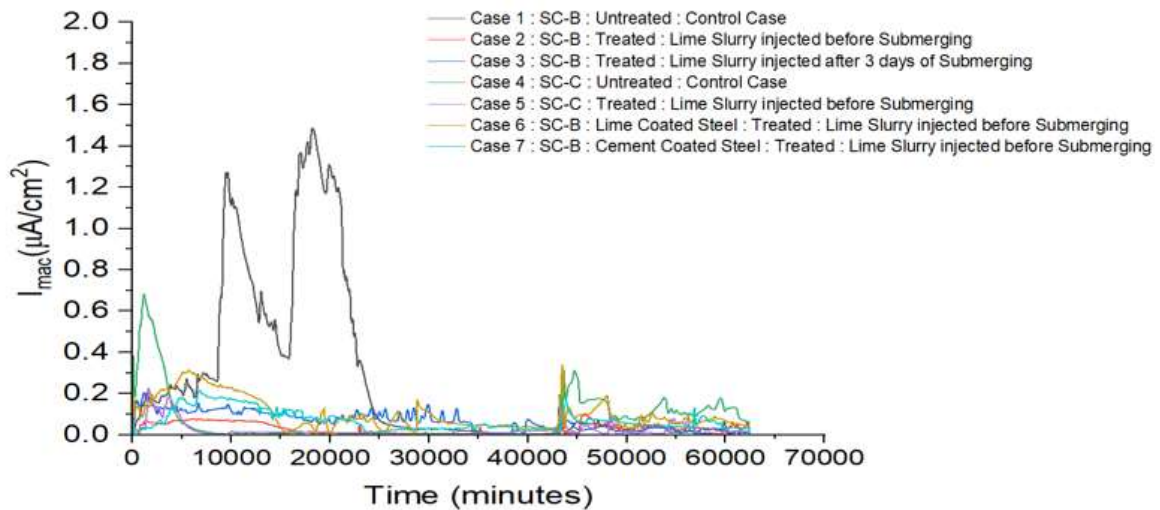


Figure 24: Macrocell Current of all cases

The macrocell current versus time of exposure graph for Cases using SC-B is shown in Fig-8. Analyzing the graph, we can conclude that the most effective treatment process is used in Case 5. Then Case 4, Case 7, Case 2, and Case 3 respectively. Using SC-C and injecting lime slurry injected before submerging in seawater is the best solution for the case investigated.

### 4.3 Depth of Corrosion:

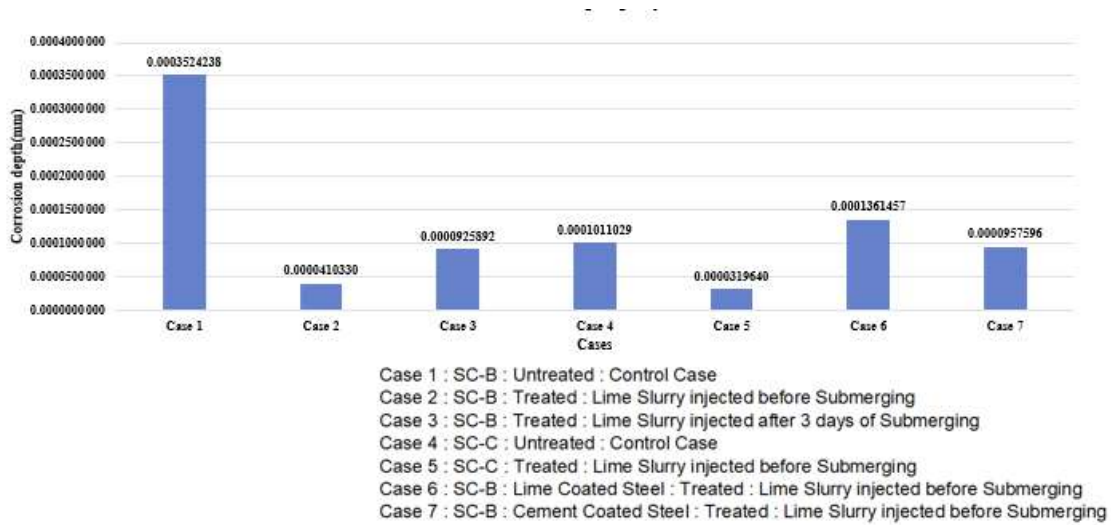


Figure 25: Depth of Corrosion

Figure 11 gives a representation of the depth of corrosion seen in different cases over a period of 60,000 minutes of an investigation. The investigation's main goal was to evaluate how different situations, including control cases and cases containing treatments or alterations, might affect corrosion behavior. The graph provides important data about the depth of corrosion that each example has endured.

Case 1, the control case using SC-B without any treatment, showed the highest corrosion depth of every case under investigation. The rebar in Case 1 had considerable levels of corrosion activity during the investigation period, as evidenced by the corrosion depth measurement of 0.0003524238 mm. Following Case 1, the graph displays the remaining cases' corrosion depths in descending order. The second-highest corrosion depth was seen in Case 6, which was followed by Case 4, Case 7, Case 3, Case 2, and lastly Case 5 with the lowest corrosion depth. Notably, Case 5 had the lowest depth of corrosion, measuring 0.0000319640 mm, and entailed treating SC-C with lime slurry. This finding indicates that, in contrast to other scenarios, the



treatment with lime slurry had a positive effect on lowering the corrosion activity inside the concrete sample.

#### 4.4 Concrete Resistance

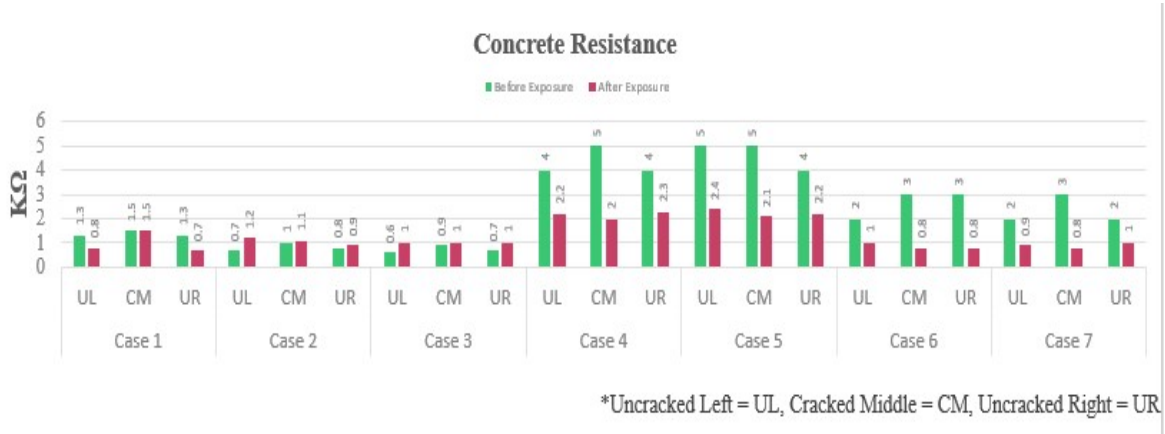


Figure 26: Corrosion Resistance in different cases

Figure 12 compares the resistance of concrete in different cases, both before and after exposure to specific conditions. The graph shows the information on the resistance values obtained in the uncracked left, cracked middle, and uncracked right areas of the concrete samples. The results indicate important distinctions between the cases, especially when contrasting the use of SC-C in Cases 4 and 5 with that of SC-B in the other cases.

The concrete resistance values in all three locations are seen to be quite similar in all cases before exposure conditions. This suggests that the concrete specimens in each case initially have similar resistance properties. But after exposure condition, in the cracked middle the concrete resistance values are higher than the uncracked left and right in all cases.

## 4.5 Half-Cell Potential

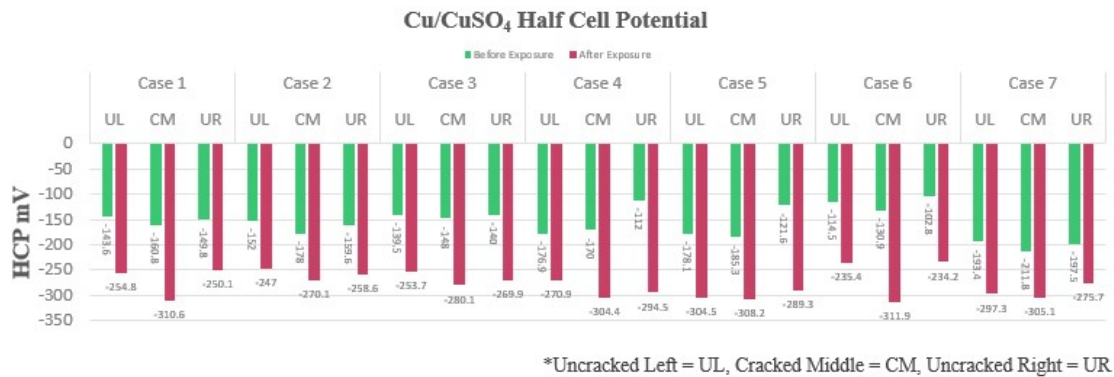


Figure 27: Half Cell Potential in different cases

The half-cell potential (HCP) measurements in various cases both before and after exposure condition are insightfully shown in Figure 12. Using a Cu/CuSO<sub>4</sub> half-cell, the HCP values were measured in three different areas: Uncracked left, Uncracked center, and Uncracked right.

When analyzing the graph, it is clear that the HCP values in every case after exposure condition showed a significant increase when compared to the values obtained before exposure. This finding suggests that the concrete samples' electrochemical behavior was significantly influenced by the exposure in seawater.

The graph also shows that, after exposure conditions, the HCP values in the Cracked middle area were higher than those in the Uncracked left and Uncracked right regions in every case. According to this, the cracked region acted as the anode and showed a larger potential, whilst the uncracked regions acted as the cathode and showed significantly lower potential values.

The phenomena wherein the cracked region acts as the anode and the uncracked region acts as the cathode is consistent with the theories underlying galvanic corrosion. When two distinct metals or regions within a material encounter differing electrical potentials, which causes the flow of electric current between them, galvanic corrosion takes place. The cracks in the

concrete act as a passageway for moisture and ions to enter the concrete matrix. Due to the moisture and ions present in saltwater, localized electrochemical cells are created, with the cracked area acting as the anode and the nearby uncracked areas as the cathodes.

## 4.6 Corrosion Current Density

Table 9: Microcell corrosion Current Density in Different Cases

Cases		Case 1			Case 2			Case 3			Case 4			Case 5			Case 6			Case 7		
Cracking Description		UL	CM	UR	UL	CM	UR	UL	CM	UR	UL	CM	UR	UL	CM	UR	UL	CM	UR	UL	CM	UR
Before Exposure	( $\mu\text{A}/\text{cm}^2$ )	<0.5	<0.5	<0.5	0.5	<0.5	<0.5	<0.5	<0.5	0.9	<0.5	<0.5	0.6	0.5	<0.5	0.6	<0.5	<0.5	<0.5	<0.5	<0.5	0.5
After Exposure		<0.5	<0.5	<0.5	<0.5	<0.5	<0.5	<0.5	<0.5	<0.5	1.3	0.9	0.6	2	<0.5	0.5	0.8	0.7	0.5	<0.5	<0.5	0.6

The corrosion current density measurements in every case, both before and after exposure conditions, are shown in detail in Table 2. The Uncracked left, cracked middle, and Uncracked right regions were each given a different corrosion current density value.

It is clear from the analysis that, prior to exposure conditions, the corrosion current density values remained at or below  $0.5 \mu\text{A}/\text{cm}^2$  in all cases and regions. Consistently, the range of values between 0 and  $0.5 \mu\text{A}/\text{cm}^2$  was recorded. These low values show that the concrete specimens at this stage have negligible corrosion activity. However, it was found that some

corrosion current density values were above the  $0.5 \mu\text{A}/\text{cm}^2$  threshold following exposure conditions. The values measured were within a range of  $0.5$  and  $2 \mu\text{A}/\text{cm}^2$ . Compared to the before exposure condition, this implies a higher amount of corrosion activity, while it is still considered to be at a relatively low level. It means low corrosion.

# **CHAPTER 5: CONCLUSION AND RECOMMENDATION**

## **5.1 General**

The primary objective of this study was to determine control procedures for macrocell and microcell corrosion of steel in cracked concrete in the marine environment. This chapter describes the summary of the research findings based on the results and discussions in Chapter 4. Moreover, the conclusion and recommendations for this investigation are also mentioned in this chapter.

## **5.2 Conclusion**

According to the study's experimental findings, SC-C cement concrete performs better under conditions when it is submerged in seawater than SC-B cement concrete. This shows that when compared to SC-B cement concrete, SC-C cement concrete has stronger resistance to corrosion in seawater. Additionally, the use of lime treatment has produced encouraging results in the vastly reduced corrosion current. The rate of corrosion has significantly lowered as a result of lime treatment applied to the concrete. The study also discovered that SC-B cement concrete bars coated with cement or lime perform better than regular bars when submerged in seawater. This suggests that adding cement- or lime-coated bars might improve SC-B cement concrete's corrosion resistance when exposed to saltwater.

Additionally, another conclusion is that lime treatment before immersing SC-C cement concrete in seawater is the most efficient treatment against corrosion among all the cases investigated. This emphasizes the significance of SC-C cement concrete receiving lime treatment as a preventative strategy to obtain the best corrosion protection in seawater conditions. Interesting results on the distribution of corrosion in cracked and uncracked regions were also found by the study. The cracked region's half-cell potential (HCP) magnitude was discovered to be greater than the uncracked regions. This suggests that the uncracked region acts as the cathode and the cracked region as the anode, where corrosion occurs.

Finally, the study found that microcell corrosion values were extremely low, indicating that microcell corrosion is minimal under experimental conditions. This suggests that in the context of this investigation, the corrosion taking place at a smaller scale, within microcells, does not significantly contribute to the overall corrosion process.

### **5.3 Recommendation**

There are some recommendations for further study considering the study's results. It is essential to assess the absorption of chloride ions in different regions after immersing the specimens in seawater since the study did not go into detail about chloride ingress in the specimens. Due to chloride ions being known to contribute to corrosion in concrete structures exposed to marine environments, this research would be extremely helpful in determining the level of chloride attack. A more thorough assessment of the concrete under investigation's corrosion resistance and long-term durability would benefit from knowing the extent of chloride ingress.

Second, the trial only lasted 45 days, which is a really little period of time. Extending the trial time is recommended to provide a more thorough comparison and assessment of the various

concrete compositions and treatment approaches against corrosion. By doing this, it may evaluate the concrete's stability and long-term performance in the marine environment. A longer trial period would allow for a more thorough evaluation of the concrete's corrosion resistance and give a stronger foundation for formulating recommendations regarding the efficacy of various concrete types and treatments.

## REFERENCES

1. Wang, J.; Wang, Q.; Zhao, Y.; Li, P.; Ji, T.; Zou, G.; Qiao, Y.; Zhou, Z.; Wang, G.; Song, D. Research Progress of Macrocell Corrosion of Steel Rebar in Concrete. *Coatings* 2023, 13, 853. <https://doi.org/10.3390/coatings13050853>
2. Mohammed, M.S.H.S.; Raghavan, R.S.; Knight, G.M.S.; Murugesan, V. Macrocell Corrosion Studies of Coated Rebars. *Arab. J. Sci. Eng.* 2014, 39, 3535–3543.
3. Mohammed, T.U., Rahman, M., Sabbir, A. *et al.* Chloride ingress and macro-cell corrosion of steel in concrete made with recycled brick aggregate. *Front. Struct. Civ. Eng.* **15**, 1358–1371 (2021). <https://doi.org/10.1007/s11709-021-0769-x>
4. Mohammed, Tarek & Hamada, Hidenori. (2006). Corrosion of Steel Bars in Concrete with Various Steel Surface Conditions. *Aci Materials Journal*. 103. 233-242.
5. Mohammed, T., Hamada, H., Al-Manum, & Hasnat, A. (2013). Corrosion of cement paste coated steel bars in marine environment. 10.13140/2.1.1658.1448.
6. Lins, V. & Oliveira, Michele & Costa, Cíntia & Araujo, Carlos. (2019). Lime Addition Effect on Corrosion of Reinforced Mortar. *Matéria (Rio de Janeiro)*. 24. 10.1590/s1517-707620190003.0777.
7. Valcuende M, Calabuig R, Martínez-Ibernón A, Soto J. Influence of Hydrated Lime on the Chloride-Induced Reinforcement Corrosion in Eco-Efficient Concretes Made with High-Volume Fly Ash. *Materials*. 2020; 13(22):5135. <https://doi.org/10.3390/ma13225135>
8. Cao Z, Su Z, Hibino M, Goda H. Effects of Mineral Admixtures on Macrocell Corrosion Behaviors of Steel Bars in Chloride-Contaminated Concrete. August 17, 2022.



9. International Journal of Corrosion. Volume 2022, Article ID 3332123, 12 pages.  
<https://doi.org/10.1155/2022/3332123>
10. Mohammed, Tarek & Hamada, Hidenori & Yamaji, Toru. (2003). Marine Durability of 30Year Old Concrete Made with Different Cements. Journal of Advanced Concrete Technology - J ADV CONCRTECHNOL. 1.63-75.10.3151/jact.1.63.
11. Mohammed, T, Hamada, H. & Yamaji, T. (2019). Long-Term Durability of Concrete Made with Slag Cements under Marine Environment. Aci Materials Journal. 116. 10.14359/51716995.
12. Mira P., Papadakis V.G, Tsimas S. “Effect of lime putty addition on structural and durability properties of concrete, Cement and Concrete Research”, Volume 32, Issue 5, 2002, Pages 683-689, ISSN 0008-8846, [https://doi.org/10.1016/S0008-8846\(01\)00744-X](https://doi.org/10.1016/S0008-8846(01)00744-X).
13. Schießl, P. (1988). Corrosion of steel in concrete: report of the Technical Committee 60-CSC, RILEM (the International Union of Testing and Research Laboratories for Materials and Structures).
14. Gonzalez, J A, Feliu, S, Andrade, C, & Alonso, C. Comparison of rates of general corrosion and maximum pitting penetration on concrete embedded steel reinforcement. United States. [https://doi.org/10.1016/0008-8846\(95\)00006-2](https://doi.org/10.1016/0008-8846(95)00006-2)
15. Mohammed T U, Otsuki N, Hamada H, Yamaji T. Macro-cell and micro-cell corrosions of steel bars in cracked concrete exposed to marine environment. In:5th CANMET/ACI International Conference on Recent Advances in Concrete Technology. Farmington Hills, MI:ACI International, 2011: 55–169
16. Lu C, Wang W, Jiang J, Hao M. Micro-environment temperature and relative humidity response of fly ash concrete under natural climatic conditions. Advances in Cement Research, 2017, 19(6): 1–10
17. Gurdían H, García-Alcocel E, Baeza-Brotons F, Garcés P, Zornoza E. Corrosion behavior of steel reinforcement in concrete with recycled aggregates, fly ash and spent cracking catalyst. Materials (Basel), 2014, 7(4): 3176–3197

18. Nanayakkara O, Kato Y. Macro-cell corrosion in reinforcement of concrete under non-homogeneous chloride environment. *Journal of Advanced Concrete Technology*, 2009, 7(1): 31–40
19. ASTM C 39/ C39M–16. Standard Test Method for Compressive Strength of Cylindrical Concrete Specimen. West Conshohocken: ASTM International, 2016
20. Michaud V, Suderman R (1999) Solubility of Sulfates in HighSO<sub>3</sub> Clinkers Ettringite The Sometimes Host of Destruction. *American Concrete Institute SP-177*, Farmington Hills, Michigan, pp: 15-25.
21. Ormellese M, Berra M, Bolzoni F, Pastore T (2006) Corrosion inhibitors for chlorides induced corrosion in reinforced concrete structures. *Cement and Concrete Research* 36: 536-547.
22. Neville PA (1983) *Corrosion of reinforcement Concrete*. pp: 48-50.
23. Bijen J (1996) Benefits of slag and fly ash. *Construction and Building Material*. 10: 309-314.
24. López-Calvo H Z, Montes-García P, Kondratova I, Bremner T W, Thomas M D A. Epoxy-Coated Bars as Corrosion Control in Cracked Reinforced Concrete. *Materials and Corrosion*, 2012, 64(7): 599–608